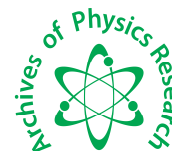




## Scholars Research Library

Archives of Physics Research, 2015, 6 (3):1-8  
(<http://scholarsresearchlibrary.com/archive.html>)



Scholars Research  
Library

ISSN : 0976-0970

CODEN (USA): APRRC7

### Growth and characterization of a new semi organic L-valine cadmium chloride monohydrate crystal

<sup>1</sup>R. Sajitha, <sup>2</sup>Bright and <sup>1</sup>Dawn Tharma Roy

<sup>1</sup>Department of Physics, N. M. Christian College, Marthandam, Tamil Nadu, India

<sup>2</sup>Department of Physics, Mar Ivanius College, Trivandrum, India

#### ABSTRACT

A new semi organic non linear optical material, L-valine cadmium chloride (LVCC crystal) has been grown successfully from aqueous solution by the conventional slow evaporation method. The grown LVCC crystal has been characterized by using powder X ray analysis and confirmed the identity of the title compound. The presence of functional groups of the grown crystal has been confirmed by Fourier Transform Infrared Spectroscopy (FTIR) analysis. The optical absorption study was examined by UV-VIS spectrum which indicates a wider optical transmission window for the grown crystal. The UV cutoff wavelength was found out as 220 nm. The work hardening coefficient has been found out as 1.0725, suggests that the given crystal belongs to moderately harder category. It is noticed that SHG efficiency of the grown LVCC crystal is 0.99 times that of the standard KDP crystal.

**Keywords:** Slow evaporation method, X-ray diffraction, Fourier Transform infrared spectrum, UV cut off wave length, work hardening co-efficient.

#### INTRODUCTION

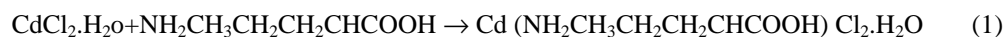
Growth of Non Linear Optical (NLO) single crystals with good quality initiates the development of many novel devices in the field of optoelectronics and optical communication such as optical modulator, optical data storage and optical switches [1-4]. Semi Organic NLO materials are generally have a high non linear coefficient, high laser damage threshold, high thermal stability and mechanical strength than inorganic crystals [5-6]. In this connection, amino acids are prominent materials for NLO applications, as they contain zwitterions, which create the hydrogen bonds used for the generation of non centro symmetry structures favorable for attractive SHG properties of crystal [7-9]. Except Glycine, generally amino acids having a Proton donating carboxyl group (Coo<sup>-</sup>) and a proton accepting amino (NH<sub>3</sub><sup>+</sup>) group, having a tendency of combining with that of inorganic salt [10]. As a result good NLO crystals such as L-Valine hydro bromide [11], L-Valine cadmium acetate [12], L-Valine Potassium Chloride [13], L-valine Zinc Sulphate [14-15], L-Valine Nickel Chloride [16], L-Valine Succinate [17], L-Valine Oxalate [18], L-Valine hydro Chloride [19], L-Valine hydro bromide [20], L-Valine Cadmium bromide [21], L-Valine Cadmium Chloride [22] has been grown and its characterization studies have been already reported.

In this present investigation, L-Valine Cadmium Chloride Crystal (LVCC) has been grown from its aqueous solution by slow evaporation method. Attempt has been made to characterize the crystals through the techniques such as powder XRD, FTIR, UV-Visible, microhardness and NLO studies.

#### MATERIALS AND METHODS

##### CRYSTAL GROWTH

L-Valine and Cadmium Chloride monohydrate has been dissolved in 1:1 equimolar ratio in deionized water using a magnetic stirrer. The chemical reaction which control the crystal growth is,



The solution was kept in undisturbed condition and allowed to crystallize by slow evaporation technique at room temperature. After 25-30 days colorless transparent crystals of LVCC were harvested. The photograph of the grown crystal is shown in Fig 3.1.



Fig.1. Photograph of the grown LVCC crystal

### CHARACTERIZATION

The LVCC crystal was subjected to powder X-ray diffraction studies powder X-ray diffraction pattern was undertaken by X-ray diffraction meter (Model JDX 8030) with  $\text{CuK}\alpha$  ( $\lambda = 1.5418\text{\AA}$ ). The presence of functional groups has been confirmed with the help of Perkin Elmer FTIR spectrometer in the range of 400 to 4000  $\text{cm}^{-1}$  using KBr pellet technique. The optical transparency range was investigated by  $\lambda$  35 model Perkin Elmer double beam uv-visible spectrometer in the range of 190nm to 1100nm. The mechanical strength of the grown LVCC crystal was studied using Reichert MD 4000E Ultra Microhardness Tester. In this method, micro indentation is made on the surface of a specimen with the help of diamond indenter. Hardness values are measured from the observed size of the impression, after a loaded indenter has penetrated and has been removed from the surface. Thus the observed hardness behavior in the final measurement of the residual impression is the summation of a number of effects involved in the materials response to the indentation pressure during loading.

### RESULTS AND DISCUSSION

#### XRD ANALYSIS

Powder X-ray diffraction study has been used for the identification of the synthesized crystals. The powdered sample was scanned in the range between 10-80 $^\circ$  at a scan rate of 2 $^\circ$ /min. The highest intense peaks of the observed powder XRD pattern has been compared with the standard XRD pattern of L-valine hydro chloride crystal (JCPDS File no -27-1899) and L-valine (JCPDS File no- 33-1954), and is analyzed. The well defined Bragg peaks at specific  $2\theta$  angles have shown high crystalline nature of LVCC crystals. The observed powder XRD of the grown LVCC crystal is shown in Fig. 1

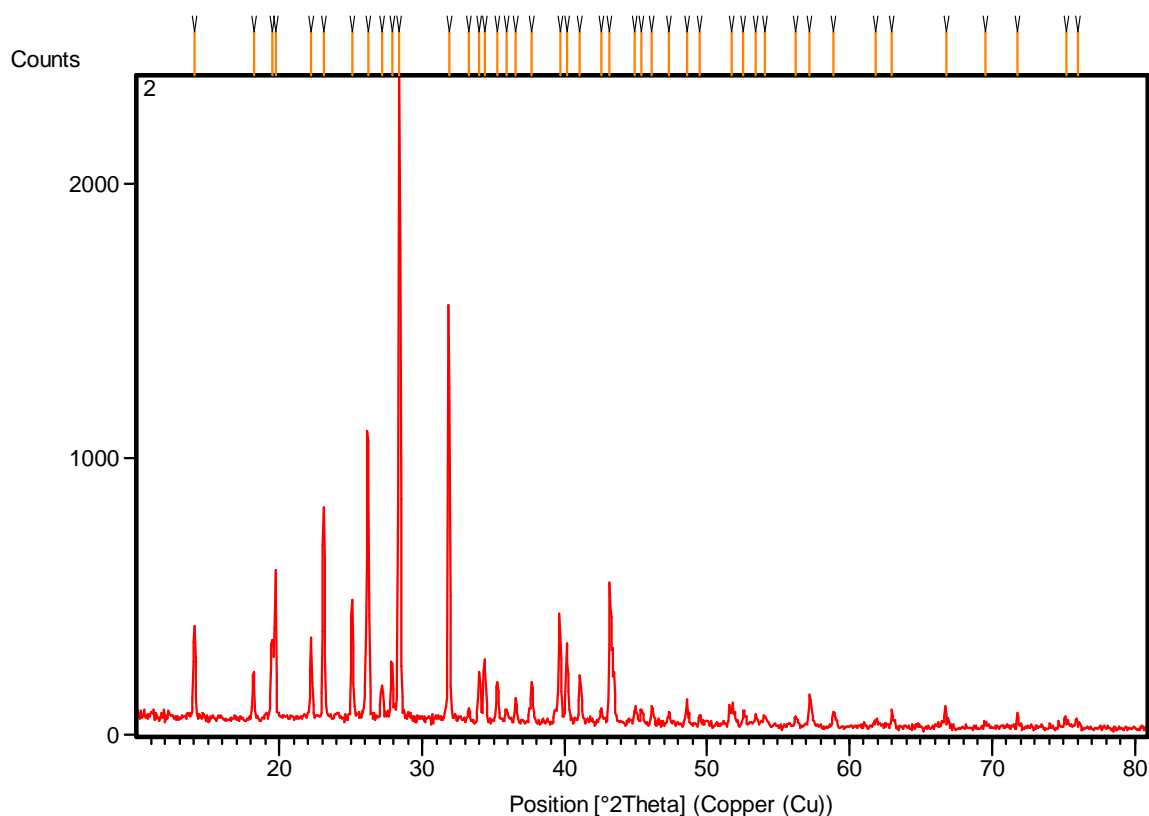


Fig. 2 Powder XRD pattern of the grown LVCC crystal

#### FTIR Analysis

The infrared spectral analysis has been used to understand the chemical bonding and functional groups present in the synthesized compound. The FTIR spectrum of LVCC crystal has been recorded in the range of  $400\text{--}4000\text{ cm}^{-1}$  using BRUKER IFS 66V model FTIR spectrometer. The FTIR spectrum of the title compound is depicted in Fig. 3.

The O-H stretching bond of water occurs at  $3786\text{ cm}^{-1}$ , which confirms the presence of water in the crystal. The observed peak at  $3425\text{ cm}^{-1}$  is due to symmetric stretching vibration of  $\text{NH}_2^+$  of L-Valine. The peak appears at  $2937\text{ cm}^{-1}$  has been attributed to  $\text{CH}_2$  asymmetric stretching vibration. The N-H-O valence stretching combination observed at  $2621\text{ cm}^{-1}$ . The peak observed at  $1589\text{ cm}^{-1}$  has been attributed to the  $\text{COO}^-$  asymmetric stretching mode of vibrations. The symmetric deformation of  $\text{NH}_3^+$  is observed at  $1507\text{ cm}^{-1}$ . The  $\text{COO}^-$  symmetric stretching bands are observed at  $1393\text{ cm}^{-1}$ . The peak of C-O stretching is assigned at  $1335\text{ cm}^{-1}$ . C-C stretching modes are observed at  $1178$  and  $1138\text{ cm}^{-1}$ . The sharp peaks at  $1063$  and  $1033\text{ cm}^{-1}$  is due to C-C -N stretching mode. The band at  $943\text{ cm}^{-1}$  is due to  $\text{CH}_2$  Rocking.  $\text{NH}_3^+$  rocking bending is positioned at  $823\text{ cm}^{-1}$ . Narrow peaks assigned at  $823\text{ cm}^{-1}$  and  $662\text{ cm}^{-1}$  are due to C-H out of plane bending. The presence of C-C Skeletal stretching peak is assigned at  $770\text{ cm}^{-1}$ .

There is an intense sharp peak at  $714\text{ cm}^{-1}$  assigned to  $\text{COO}^-$  in plane deformation. The narrow sharp peak at  $542\text{ cm}^{-1}$  and is assigned to C-CO deformation. The  $\text{COO}^-$  rocking is observed at  $431\text{ cm}^{-1}$ . The observed wave numbers obtained from the recorded spectra of the grown LVCC crystal has been found to be in good agreement with the assignments proposed for L-Valine crystal [23] and are listed in Table. 1

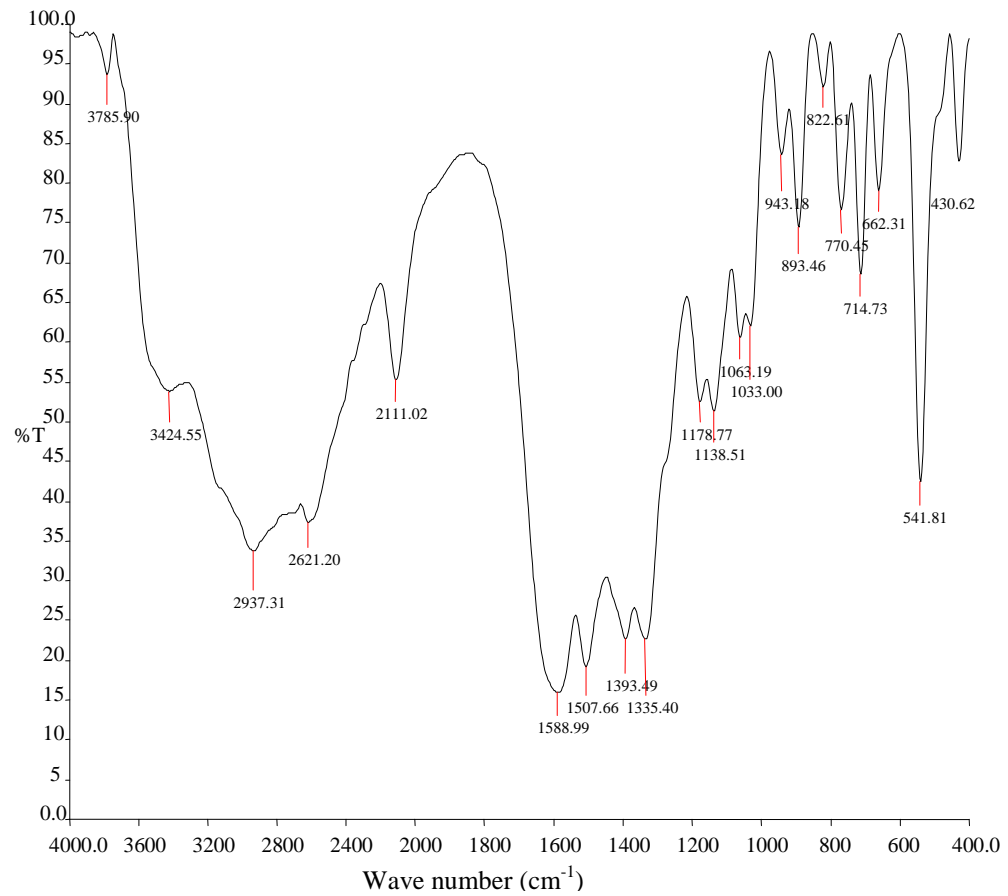
**Fig.3 FTIR spectrum of LVCC crystal**

Table.3.2. FTIR Spectral assignments of LVCC crystal

Wave number (cm <sup>-1</sup> )		Assignments
L-Valine (cm <sup>-1</sup> )	LVCC (cm <sup>-1</sup> )	
-----	3786	O-H stretching mode
2945	2937	NH <sub>2</sub> <sup>+</sup> symmetric stretching
2945	2937	CH <sub>2</sub> asymmetric stretching
2629	2621	N-H-O valance stretching combination
1585	1589	COO <sup>-</sup> asymmetric stretching
1508	1507	NH <sub>3</sub> <sup>+</sup> symmetric deformation
1396	1393	COO <sup>-</sup> symmetric stretching
1329	1335	C-O Stretching
1178	1178	C-C Stretching
1140	1138	C-C stretching
1065	1163	C-C- N stretching
1028	1033	C-C -N stretching
949	943	CH <sub>2</sub> Rocking
894	893	NH <sub>3</sub> <sup>+</sup> Rocking bending
824	823	C-H out of plane bending
775	770	C-C skeletal stretching
716	714	COO <sup>-</sup> in plane deformation
664	662	C-H out of plane bending
542	542	C-CO deformation
428	431	COO <sup>-</sup> rocking

### UV –Vis Spectral Analysis

Optical transmission spectrum for the grown LVCC crystal has good transmittance in the entire visible region and the lower uv cut off wave length is found to be 220 nm. High transmittance in the visible region with lower UV cut off wavelength shows the most favourable characteristics used as a potential candidate for NLO applications. UV-visible spectrum of LVCC crystal is shown in Fig. 4.

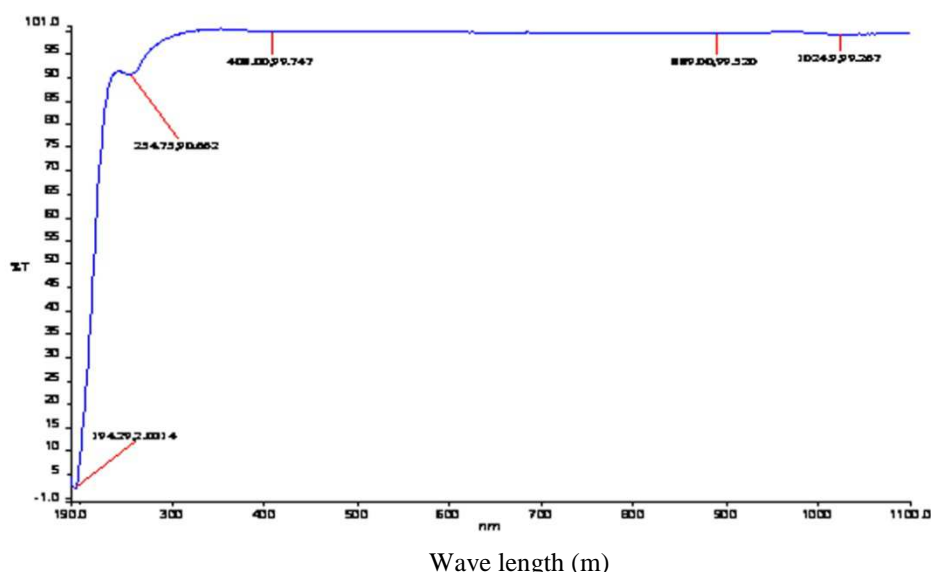


Fig.4. UV-Visible Spectrum of LVCC Crystal

### Micro Hardness Studies

Indentation hardness has been the most commonly used technique to measure the mechanical properties of the materials. It has been considered as a principal parameter for mechanical characterization of materials especially to understand the role of plastic deformation [24]. A general definition of hardness is the mechanical resistance of a solid object to permanent change [25]. The hardness is estimated from the ratio of the load applied on indenter to the area of the impression left on the specimen. Vicker's microhardness number (Hv) was determined using the relation,

$$Hv = 1.8544 P/d^2 \text{ kg/mm}^2 \quad (2)$$

A graph has been plotted between Vicker's microhardness number (Hv) and the applied load (P) is shown in Fig.5.

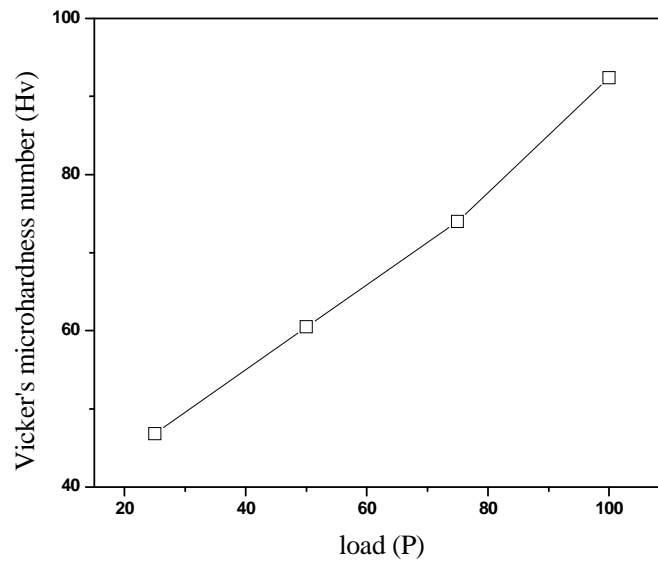


Fig. 5 The variation of Hv with the applied load for LVCC crystal

In the present study the micro hardness value has been found to increase with load up to 100g, after that cracks has been occurred, which may be due to the release of internal stresses generated with indentation. Cracking occurs above a certain load (threshold load), below this load, the indentation leads to deformation behavior, whereas above the threshold, it shows fracture behavior [27-28]. Also vacancies, dislocations and strains alter the hardness. This behavior of increasing micro hardness with the applied load is also known as reverse indentation size effect (RISE) [29]. The reverse effect is very uncommon and is usually due to softer superficial layers on the specimen surface [30]. The reverse ISE can be caused by the relative predominance of nucleation and multiplication of dislocations. The relation between load and the size of indentation is given by Meyer's law [31],

$$P = K_1 d^n \quad (3)$$

Where  $K_1$  is a constant,  $n$  is the work hardening coefficient.

On the basis of careful investigation on various substances, Onitsch [32] has been found that the value of  $n$  lies between 1-1.6 for hard materials and more than 1.6 for soft ones. The value of  $n$  has been estimated from the plot of  $\log p$  versus  $\log d$  (Fig.6), and has been found out as 1.0725 for the grown LVCC crystals, suggests that it belongs to the moderately harder category. The intercept of the above plot gives the value of  $K_1$ , the standard hardness.

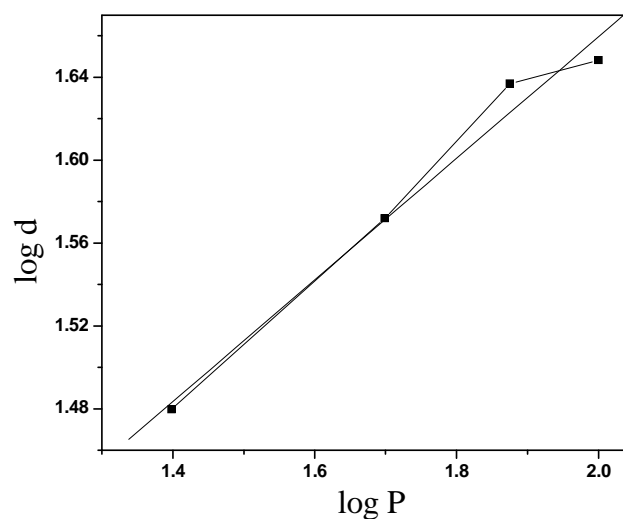


Fig. 6 The plot of log p vs log d for LVCC crystal

After the load is removed it has been argued that the area may be susceptible to elastic recovery. The specimen undergoes relaxation involving a release of the indentation stress away from the indentation site. This leads to a larger indentation size and hence to a lower hardness at low loads [33]. When elastic recovery is associated with indentation,

$$P = K_2 (d+x)^2 \quad (4)$$

Where  $K_2$  is load independent constant and  $x$  is the correction factor [34].

Simplifying Eqs. (3) and Eqs.(4)

$$d^{n/2} = (K_2/K_1)^{1/n} d + (K_2/K_1)^{1/n} x \quad (5)$$

Plotting  $d^{n/2}$  against  $d$  should yield the slope  $(K_2/K_1)$  and the intercept gives  $x$  (Fig.7).

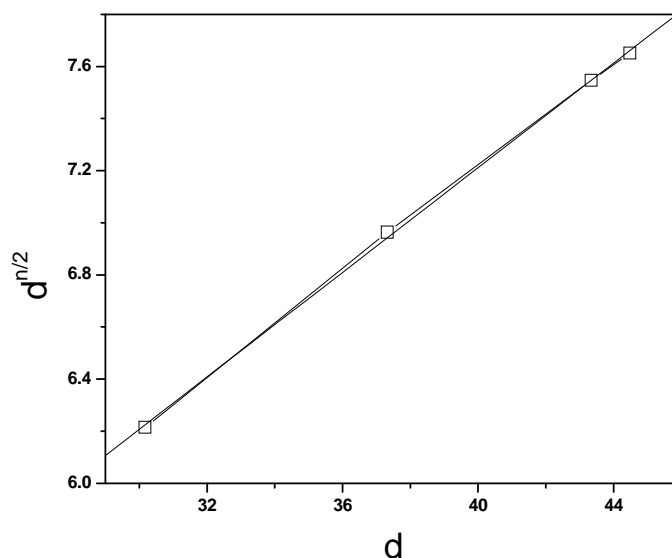


Fig. 7 Plot of  $d$  vs  $d^{n/2}$  for LVCC crystal

The micro hardness parameters of LVCC crystal are listed in Table. 1

n	K1(kg/m)	K2(kg/m)	X( $\mu$ m)
1.0742	0.2936	2.997	0.10038

## NLO STUDIES

The NLO property of LVCC crystal has been assessed by the Kurtz powder technique [35]. The sample was illuminated using Q-switched Nd: YAG laser with the first harmonic output of 1064nm and pulse width of 8ns. The emission of green radiation from the crystal confirmed existence of second harmonic generation. The second harmonic generation signal of 8.74 mJ for LVCC crystal was obtained for an input energy of 0.68J. But the standard KDP crystal has given an SHG signal of 8.8mJ for the same input energy. Thus it is noticed that SHG efficiency of the grown LVCC crystal is 0.99 times that of the standard KDP crystal.

## CONCLUSION

The title compound L-Valine Cadmium Chloride (LVCC) crystal has been grown by the conventional slow evaporation technique. The sharp peaks from the observed powder XRD pattern of LVCC crystal confirmed the crystalline nature. The functional groups present in the compound has been explained on the basis of FTIR studies. The UV cutoff wave length has been found out as 220 nm. The work hardening coefficient has been found out as 1.0725, suggests that the grown crystal belongs to moderately harder one. The SHG efficiency of the grown LVCC crystal is 0.99 times that of the standard KDP crystal.

## REFERENCES

- [1] V.G.Dmitriev, G.G.Gurzadyan, D.N.Nicogosyan, Hand book of Non-Linear Optical Crystals, Springer Verlag, New York, **1999**.
- [2] M.S.Wong, C.Bosshard, F.Pan, P.Gunter, *Adv.Material*, **1996**, 8, 677.
- [3] M.G.Popadopoulos, J.Leszczynski, A.J. Sadler, Non-Linear Optical Properties of Matter : From Molecules to Condensed Phases, Kluwer, Dordrecht, **2006**.
- [4] H.S.Nalwa, S.Miyata, Non-Linear Optics of Organic Molecules and Polymers, CRC Press, Boca Raton, **1997**.
- [5] J.Zyss, J.F.Nicoud, M.J.Coquillay, *J.Chem. Phys.*, **1984**, 81, 4160.
- [6] R.A.Hann, D.Bloor, Organic Materials for Non-linear Optics, Special Publication, The Royal Society of Chemistry, London, **1989**.
- [7] M.H.Jiang, Q.Fang, *Adv. Materials*, **1999**, 11, 1147.
- [8] C.Justin Raj, S.Dinakaran, S.Krishnan, B.Milton Boaz, R.Robert, S.Jerome Das, *Optical Communication*, **2008**, 281, 2285.
- [9] M.Lydia, Caroline, A.Kandaswamy, R.Mohan, S.Vasudevan, *J.Cryst. Growth* **2009**, 211, 1161.
- [10] K.Kirubavathi, K.Selvaraju, R.Valluvan, N.Vijayan, S.Kumararaman, *Spectrochim. Acta A* **2008**, 69, 1283.
- [11] S.Moitra, T.Kar, *J.Crys. Growth*, **2008**, 310, 4539.
- [12] J.Chandra Sekaran, P. Ilayabarathi, P.Madeswaran optics Communication.
- [13] J. Chandrasekaran, P.Ilayabaruthi, P.Maadeswaran, *Rasayan J.Chem*, **2011**, 4,320.
- [14] Bikshandarkoil, R.Srinivasan, Rita , N.Jyai, *Spectro Chimica Acta part A: Molecular and Biomolecular Spectroscopy*, **2014**, 120, 621.
- [15] A Puhaj Raj, C.Rama Chandra Raja, *Spectro Chimica Acta Part A: Molecular and Bio Molecular Spectroscopy*, **2012**, 97, 83.
- [16] M.K.Sangeetha, M.Mariappan, G.Madurambal, S.C.Mojumdar, *J.Therm. Anal. Calorim* **2012**, 108, 887.
- [17] C.Ramachandra Raja, A.Antony Joseph, *Spectro Chimica Acta part A: Molecular and Biomolecular Spectroscopy* **2009**, 74, 825.
- [18] Deepa Janana Kumar, P.Mani, *Int. J. Chem, Tech. Research* **2013**, 4, 1679.
- [19] S.Moitra, S.K.Seth, T.Kar, *J.Crys. Growth* **2010**, 312, 1977.
- [20] R.Parthasarathy, R.Chandra Sekaran, *Ind.J.Pure and App. Phys.* **1966**, 4, 293.
- [21] J.Chandrasekaran, P.Ilaya Bharathi, P.Matheswaran, P.Mohammed Kutti, S.Pari, *Optik-Int. J. for Light and electron Optics*, **2012**, 123, 1407.
- [22] P. Maadeswaran, J.Chandrasekaran, *Optik – Int. J.for light and electron optics*, **2011**, 122, 1128.
- [23] E.Ramachandran, S.Natarajan, *Crys, Res. Tech.*, **2009**, 44, 641.
- [24] O.Sahin, O.Uzun, U.Kolemen and N.Ucar, *Mat. Characterization*, **2008**, 59, 427.
- [25] Morten M.Smedskjaer, Martin Jensen, and Yuan Zheng Yue, *J.Am.Ceram. Soc.***2008**, 91, 514.
- [26] Bernard William Mott, *Microindentation Hardness Testing*, Butter worths, London, **1956**.
- [27] B.R.Lawn and A.G.Evans, *J.Mater. Sci.* **1977**, 12, 2195.
- [28] B.R.Lawn and D.B.Marshall, *J.Am. Ceramic Soc.* **1979**, 62, 347
- [29] H.L. Neil, *Hardness and Hardness Measurements*, 2<sup>nd</sup> ed. Chapman and Hall Ltd., London, **1967**.
- [30] Philip M.Sargent, *J.Mater. Sci. Letter*, **1989**, 8, 1139.
- [31] E.Meyer, *Z.ver, Dtsch. Ing.*, **1908**, 52, 645.
- [32] E. M. Onitsch, *Microskopie*, **1947**, 2, 131
- [33] K.Sangwal, *Mat. Chem. and Phys.* **2000**, 63, 145-152.
- [34] J.Benet Charles, *Mat. Chem. and Phys.* **1996**, 45, 189.
- [35] S. K. Kurtz, T. T. Perry, *J. Appl. Phys.* **1968**, 39, 3798.